SPE-190256-MS

Solvent Leakoff During Gel Placement in Fractures: Extension to Oil-Saturated Porous Media

B. Brattekås, The National IOR Centre of Norway, University of Stavanger; G. Ersland, University of Bergen; R. S. Seright, New Mexico Institute of Mining and Technology

Copyright 2018, Society of Petroleum Engineers

This paper was prepared for presentation at the SPE Improved Oil Recovery Conference held in Tulsa, Oklahoma, USA, 14-18 April 2018.

This paper was selected for presentation by an SPE program committee following review of information contained in an abstract submitted by the author(s). Contents of the paper have not been reviewed by the Society of Petroleum Engineers and are subject to correction by the author(s). The material does not necessarily reflect any position of the Society of Petroleum Engineers, its officers, or members. Electronic reproduction, distribution, or storage of any part of this paper without the written consent of the Society of Petroleum Engineers is prohibited. Permission to reproduce in print is restricted to an abstract of not more than 300 words; illustrations may not be copied. The abstract must contain conspicuous acknowledgment of SPE copyright.

Abstract

Crosslinked polymers extrude through fractures during placement of many conformance improvement treatments, as well as during hydraulic fracturing. Dehydration of polymer gel during extrusion through fractures has often been observed, and was extensively investigated during the last decades. Injection of highly-viscous gel increases the pressure in a fracture, which promotes gel dehydration by solvent leakoff into the adjacent matrix. The present comprehension of gel behavior dictates that the rate of solvent leakoff will be controlled by the gel and fracture properties, and to a less extent impacted by the properties of an adjacent porous medium. However; several experimental results, presented in this work, indicate that solvent leakoff deviates from expected behavior when oil is present in the fracture-adjacent matrix. We investigated solvent leakoff from Cr(III)-Acetate-HPAM gels during extrusion through oil-saturated, fractured core plugs. The matrix properties were varied to evaluate the impact of pore size, permeability and heterogeneity on gel dehydration and solvent leakoff rate. A deviating leakoff behavior during gel propagation through fractured, oil-saturated core plugs was observed, associated with the formation of a capillary driven displacement front in the matrix. Magnetic Resonance Imaging (MRI) was used to image water leakoff in a fractured, oil-saturated carbonate core plug and verified the position and existence of a stable displacement front. The use of MRI also identified the presence of wormholes in the gel, during and after gel placement, which supports gel behavior similar to the previously proposed Seright filter-cake model. An explanation is offered for when the matrix impacts gel dehydration and supported by imaging. Our results show that the properties of a reservoir rock may impact gel dehydration; which, in turn, strongly impacts the depth of gel penetration into a fracture network, and the gel strength during chase floods.

Introduction

Polymer gel treatments have been investigated by the oil industry for decades, due to their usefulness in both enhanced oil recovery (EOR) and hydraulic fracturing. In EOR processes, the presence of highly viscous polymer gel in the fracture network reduced the conductivity of fractures, and provided improved pressure drops and increased sweep efficiency within the rock matrix during chase floods [Hild and Wackowski (1999), Kantzas et al. (1999), Sydansk and Southwell (2000), Seright et al. (2003), Portwood (2005),

Willhite and Pancake (2008)]. In hydraulic fracturing, polymer gel is used as a fracturing fluid, to open fractures and transport propping agents along the fracture length (Dantas, Santanna et al. 2005).

Many commonly used polymer gels (e.g. the Cr(III)-acetate-HPAM gel used in this work) lose water (dehydrate) during extrusion through fractures. Gel dehydration, also termed *leakoff*, was observed and quantified during gel propagation through fractures in several previous publications [e.g. Seright (1995, 1999, 2001, 2003a, b) and Brattekås et al. (2015)]. Water leakoff from gel controlled the rate of gel propagation into a reservoir (Seright 2003a), as well as the rate of fracture growth during hydraulic fracturing [Howard and Fast (1957, 1970), Penny and Conway (1989)]. When leakoff occurs during gel injection, a higher volume of gel is required to reach a given distance in the reservoir than anticipated from the fracture volume. A high degree of leakoff reduces the efficiency of hydraulic fracturing (Howard and Fast 1957). Leakoff also increases the gel concentration and resistance to washout (Brattekås et al. 2015), which can improve the gel fracture blocking ability during subsequent EOR injections. Regardless of the purpose of the polymer gel treatment, an accurate understanding and description of leakoff in fracture systems is necessary.

Water leakoff has been described by two models: the Carter model [Howard and Fast (1957, 1970), Penny and Conway (1989)] and the alternative Seright model (Seright 2003a), which represent the present comprehension of gel behavior during injection. The models propose that the rate of water leakoff is controlled by gel and fracture properties, and to a less extent impacted by the properties of an adjacent porous medium. The Carter and Seright models are similar on a macroscopic scale, i.e. the rate of water leakoff linearly decreases when plotted versus time on a log-log plot (**Figure 1**). The leakoff rate will be further discussed in the present work. The two models are, however, fundamentally different in terms of gel behavior during placement. In particular, the models describe the formation of a concentrated gel filter-cake in the fracture differently (**Figure 1**). An important assumption in the Carter model is that the filter-cake forms uniformly on the fracture surface during water leakoff, i.e. the thickness of the filter cake on the fracture faces was uniform at any given time. Seright proposed the formation of an aerially and volumetrically heterogeneous filter cake, forming when fragments of injected gel dehydrated and settled in the vicinity of where the dehydration occurred (i.e., the filter-cake was non-uniformly distributed in the fracture volume). Recent advances in *in-situ* imaging supported the existence of a randomly distributed filter-cake in the fracture volume (Brattekås et al. 2016).

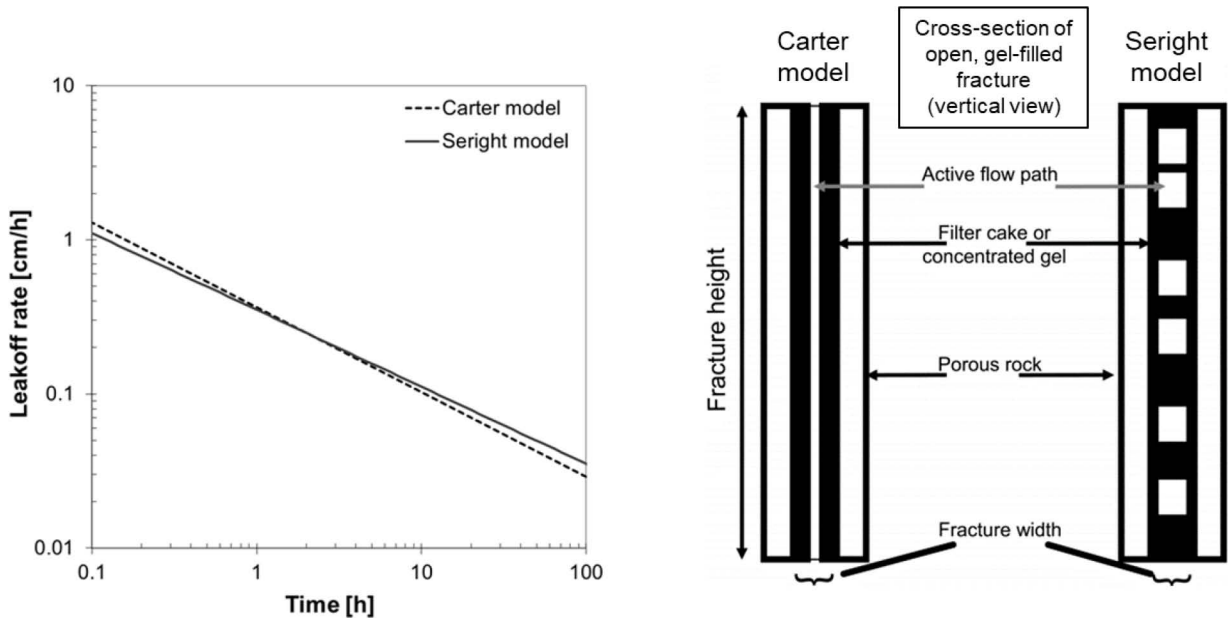

Figure 1—Two common models used to predict fluid leakoff from polymer gel: the leakoff model by Carter and the alternative leakoff model by Seright. *Left:*The macroscopic behavior of gel, i.e. leakoff rates versus time, are similar in both models. *Right*: Filter cake formation differs significantly between the two models (figure modified from Seright 2003a).

The leakoff rates predicted by the Seright model are based on experimental work, where gel was injected into longitudinal fractures through porous rock core plugs. The core plugs were saturated by water corresponding with the water bound in gel (the gel solvent). In rocks saturated by water only, saturation functions (capillary pressure and relative permeability) are not present in the matrix, and consequently, do not affect gel placement.

Saturation functions are, however, important when considering fractured hydrocarbon reservoirs, where oil is also present in the rock matrix. We investigated water leakoff from Cr(III)-Acetate-HPAM gels during extrusion through oil-saturated, fractured core plugs. The work presented in this paper was motivated by an attempt to understand when (and if) the properties of the rock matrix influence water leakoff, and why and when the measured leakoff properties deviates from expected behavior.

Experiments

Core preparations

Cylindrical core plugs were drilled from large outcrop rock blocks of different core materials:

1. Rørdal chalk from Aalborg in Denmark [Ekdale and Bromley (1993), Hjuler and Fabricius (2007)], where the porosity and absolute permeability values for core plugs used in this work ranged from ϕ =43-46% and K = 3-10mD, respectively. Rørdal chalk has small pore throats and is expected to be homogeneous.
2. Edwards limestone from west Texas, USA [Tie (2006), Johannesen (2008)]. Trimodal pore sizes, vugs and microporosity have been identified in this core material. A variation in porosity and permeability values, ranging between ϕ = 16-24% and K = 3-28mD, was found to be representative for the large rock block from which cores were drilled for this work.
3. Bentheimer sandstone from Bentheim, Germany [Schutjens et al. (1995), Klein and Reuschle (2003)] is a homogeneous sandstone with large pore throats and porosity and absolute permeability values averaging at ϕ = 23% and K =1100mD.

The cores were cut to length (5-15 cm), and a band saw was used to create smooth, longitudinal fractures through each core plug. The cores were assembled with open fractures; POM (Polyoxymethylene) spacers were placed along the top and bottom of the fracture to maintain a constant fracture aperture of 1mm. Some cores were assembled with different rock materials on each side of the fracture (e.g., a Rørdal chalk core half was assembled together with a Bentheimer sandstone core half or an Edwards limestone core half to create a contrast in properties on each side of the fracture). The core circumference and outlet end faces were covered in several layers of epoxy, to prevent flow and to enable the cores to withstand elevated pressures. The inlet end faces were left open to flow. POM end pieces were glued to the inlet and outlet end face. Holes were drilled through the epoxy 1 cm from the outlet end face of each core half. Short pieces of 1/8'' stainless steel tubing were positioned into the holes and glued in place, to be used as matrix production outlets. Core 8RC was placed in an MRI for imaging of gel placement, thus stainless-steel tubing pieces were omitted. Core 8RC features a specially designed POM end piece at the outlet end face, facilitating three production outlets; one for the fracture and one for each core half. The core plug properties may be found in **Table 1**.

Table 1—Core properties.

Core ID	K_{ratio}	Core half	Core material	L [cm]	H [cm]	r_{max} [cm]	Porosity [%]	PV [ml]
1EDW	1	CH1	Edwards limestone	7.18	4.78	2.12	25.5	12.9
		CH2	Edwards limestone	7.18	4.78	2.28	25.5	15.1
2BS	1	CH1	Bentheimer Sandstone	6.94	4.91	2.24	23.0	15.0
		CH2	Bentheimer Sandstone	6.94	4.92	2.41	23.0	15.2
3PC	1	CH1	Rørdal chalk	8.63	3.79	1.76	46.0	19.3
		CH2	Rørdal chalk	8.61	3.79	1.84	46.0	21.1
4BS-EDW	39	CH1	Bentheimer Sandstone	7.3	5.16	2.54	30.0	22.3
		CH2	Edwards limestone	7.19	4.88	2.34	27.0	16.8
5BS-EDW	86	CH1	Bentheimer Sandstone	7.40	5.14	2.54	30.0	21.9
		CH2	Edwards limestone	7.27	4.91	2.53	21.0	15.5
6EDW-RC	10	CH1	Rørdal chalk	5.95	5.08	2.43	46.0	25.8
		CH2	Edwards limestone	5.90	4.88	2.36	40.0	19.7
7BS-RC	183	CH1	Rørdal chalk	6.04	5.07	2.52	45.0	27.4
		CH2	Bentheimer Sandstone	5.57	5.11	2.53	23.0	13.3
8RC	1	CH1	Rørdal chalk	7.61	4.92	2.34	46.6	35.6
		CH2	Rørdal chalk	7.61	4.91	2.34	46.6	35.6

The core preparation procedure required the core material to be dry during assembly (for two reasons: 1) the epoxy glue did not stick well to wet surfaces, and 2) the procedure took several hours/days to complete, during which time saturated core plugs were prone to significant evaporation and associated uncertainties). The length (L), fracture height (H) and the maximum thickness (r_{max}) was measured for each core half before assembly. All cores were saturated directly with mineral oil (n-decane) under vacuum, after finalized assembly. The n-Decane was filtered through glass wool and silica gel before use, to remove polar components, and should not influence core wettability, which is assumed to be strongly water-wet in this study. Average porosities and pore volumes were determined from weight measurements. In cores where the core halves were of different core materials, porosities and pore volumes were estimated using a simple matching procedure; the total pore volume for the system, provided from weight measurements, was corrected for fracture and tubing volumes. The porosities of core half 1 (CH1) and core half 2 (CH2) were adjusted within the ranges specified above, until the sum of the calculated pore volumes corresponded to the total pore volume. The permeability contrast for each system (K_{ratio}) was approximated using assumed absolute permeability values of 6 mD and 1100 mD for chalk and sandstone, respectively, while Edwards limestone permeabilities were estimated from porosity using a linear approximation (Haugen et al. 2008).

Gel injection

5000 ppm of HPAM polymer (5 million Daltons molecular weight, degree of hydrolysis 10-15%) was mixed in brine (4wt% NaCl, 3.4wt% $CaCl_2$, 0.5wt% MgCl, 0.05wt% NaN_3) until completely dissolved, and 417-ppm Cr(III)-acetate crosslinker was added to the solution to make gelant. The gelant was placed in an accumulator at an elevated temperature of 41°C for 24 hours (~ five times the gelation time) to form gel. The crosslinked polymer gel was cooled to ambient conditions (~ 23°C), before injection into the open fractures. The gel used for core 8RC was based on D_2O-brine, but followed the same procedure. Brattekås

et al. (2015) injected Cr(III) acetate-polyacrylamide gel into fractured, cylindrical core plugs of the same chalk and sandstone core material as used in the present work. Their cores were fully water saturated at initiation of gel injection. Gel injection rates of 200 mL/h and above yielded leakoff rates that followed the Seright model (i.e., the gel behaved as predicted during injection). A gel injection rate of 200 mL/h was therefore chosen for the present experiments, where the core plugs were fully oil-saturated at the start of gel injection. Gel injection continued for approximately four hours (~ 800 mL of gel). The fracture volume (FV) ranged from 3-4 mL; hence, more than 200 FV of formed gel was extruded through the core plugs in these experiments. The injection pressure at the fracture inlet and effluents from each core half, produced through the matrix production outlets, were measured with time during gel injection. The experimental setup is shown in **Figure 2**. Core 8RC was placed in an MRI for imaging during gel injection and the experimental setup, shown in **Figure 3**, therefore differed slightly from the other experiments.

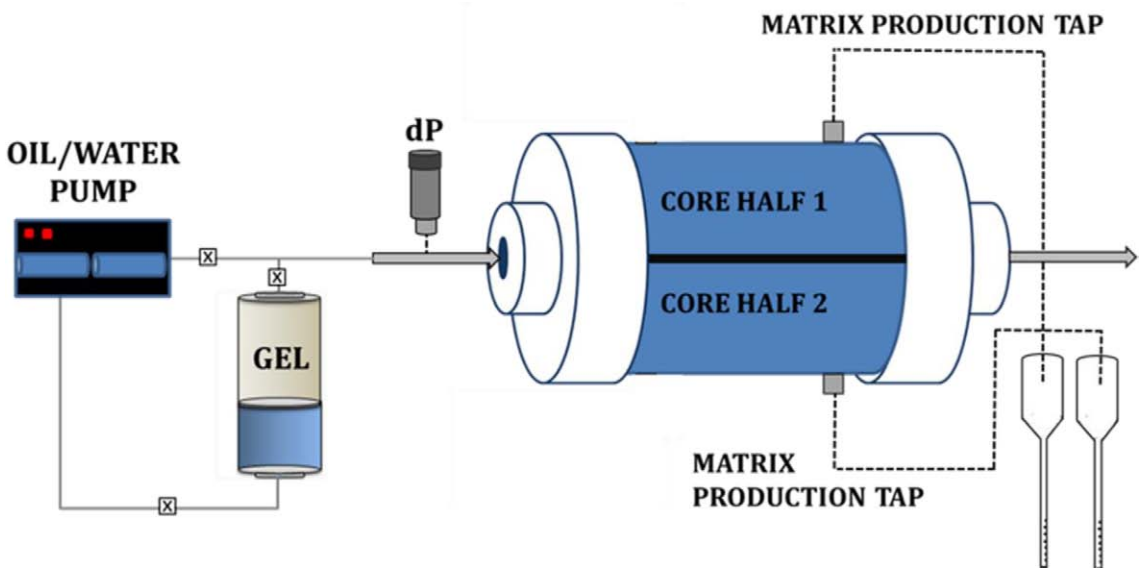

Figure 2—Schematic experimental setup for gel injection into fractured cores. The fluids produced from each core half were logged separately versus time.

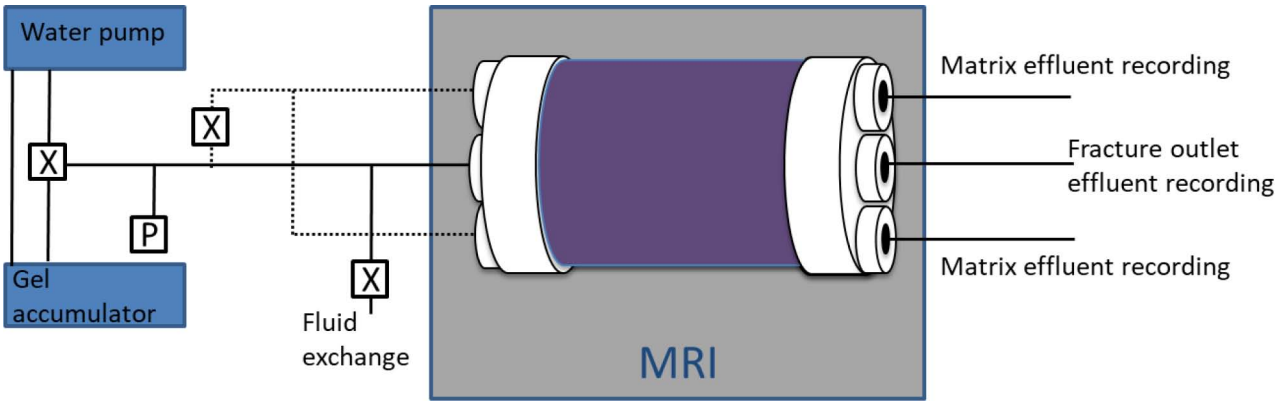

Figure 3—Experimental setup for core 8RC, placed in an MRI during injection of D_2O-based polymer gel.

Results and Discussion

Gel injection into fractured, oil-saturated core plugs

The water leakoff rate during gel injection is commonly calculated based on measurements of the produced effluent volume through a rock matrix (both in this and previous experimental papers): the effluent volumes

were logged versus time (both oil and water were produced through the matrix in this work), and divided by the fracture surface area and time interval between measurements to calculate the leakoff rate. Due to different core material on each side of the fracture in many of the experiments (**Table 1**), produced fluids were measured separately for each core half in this work. Based on the volume of oil produced from each core half versus time, we expected to be able to calculate the saturation development in each core half. In cores with a permeability contrast between the core halves, this was, however, not straight forward. Due to gel dehydration, several fracture volumes of gel must be injected before gel breakthrough is observed at the producing end (termed *outlet*) of the core. During this time, we observed either: 1) production of more than one fracture volume of oil from the fracture production outlet. Some of this oil originates from the matrix, but cannot be assigned to a specific core half in opaque systems. 2) No oil production from the fracture outlet, but significant oil production from the more permeable core half (total volume of oil produced through one matrix production outlet frequently exceeding the pore volume of the core half). These artifacts, associated with the use of small core plugs with a strong water-wetting preference, yielded direct calculations of saturation challenging; thus, normalized water saturation developments are given in the figures in this section (saturations were normalized to the total volume of oil produced from the respective matrix production outlet).

Sandstone. Formed polymer gel was injected into oil-saturated Bentheimer sandstone cores. Due to large pore throats, associated high permeability and low capillarity was expected for this core material. **Figure 4** shows leakoff rates calculated from effluent recordings during gel injection into 2BS (both core halves sandstone) and composite cores: sandstone core halves assembled with another core material on the opposite side of the fracture (chalk in core 7BS_RC, limestone in cores 4BS_EDW and 5BS_EDW).

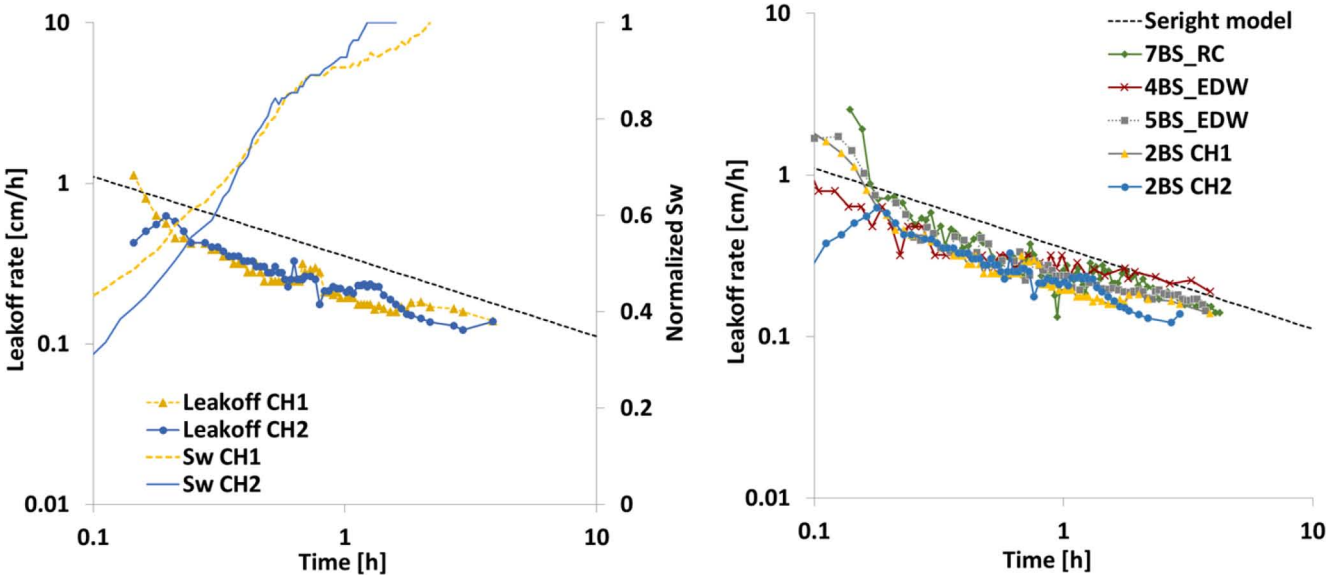

Figure 4—Effluents produced from sandstone core halves during gel injection formed the basis for leakoff rate calculations. ***Left:*** **Water leakoff rate in core 2BS, where both core halves were of sandstone material.** ***Right:*** **Leakoff rates for all sandstone core halves: sandstone coupled with sandstone, limestone and chalk.**

The leakoff rates decreased linearly on a log-log plot, slightly below the Seright leakoff model. The type of core material on the opposite side of the fracture did not impact the leakoff rates through the sandstone core halves, although the volume of oil produced through the sandstone varied, and was higher when sandstone was assembled with chalk. The small reduction in leakoff rate compared to the Seright model will be discussed in another section (***Gel dehydration on the core scale***, page 15).

Limestone. A trimodal pore size distribution, with both microporosity and vugs, was identified in previous studies of the Edwards limestone core material (Johannesen, 2008), thus significant local variations in permeability and capillarity may be expected. Effluents produced from each matrix production outlet during gel injection formed the basis for leakoff calculations. Leakoff rates for limestone core halves are shown in **Figure 5**, and deviated from the expected results (i.e., the Seright model). During early-stage gel injection, oil was produced from the matrix production outlets and the leakoff rates decreased similar to the Seright model, exhibiting a nearly linear trend on a logarithmic rate/time plot. At the start of two-phase production (oil and water) from the matrix production outlets, a swift decrease in leakoff rate was observed. After the production of oil ceased, only water was produced from the matrix outlets and a nearly constant leakoff rate was measured for the remaining gel injection. This trend was similar for all limestone core halves: both when the same core material was used on each side of the fracture (core 1EDW in **Figure 5**), and when limestone was assembled with sandstone (4BS_EDW and 5BS_EDW) or chalk (6EDW_RC) on the opposite side of the fracture. The leakoff rate plateau (nearly constant leakoff rate observed when water was produced alone through the matrix outlets) varied between core halves regardless of the core material with which limestone was assembled. This may be explained by the inherent heterogeneity of the limestone core material.

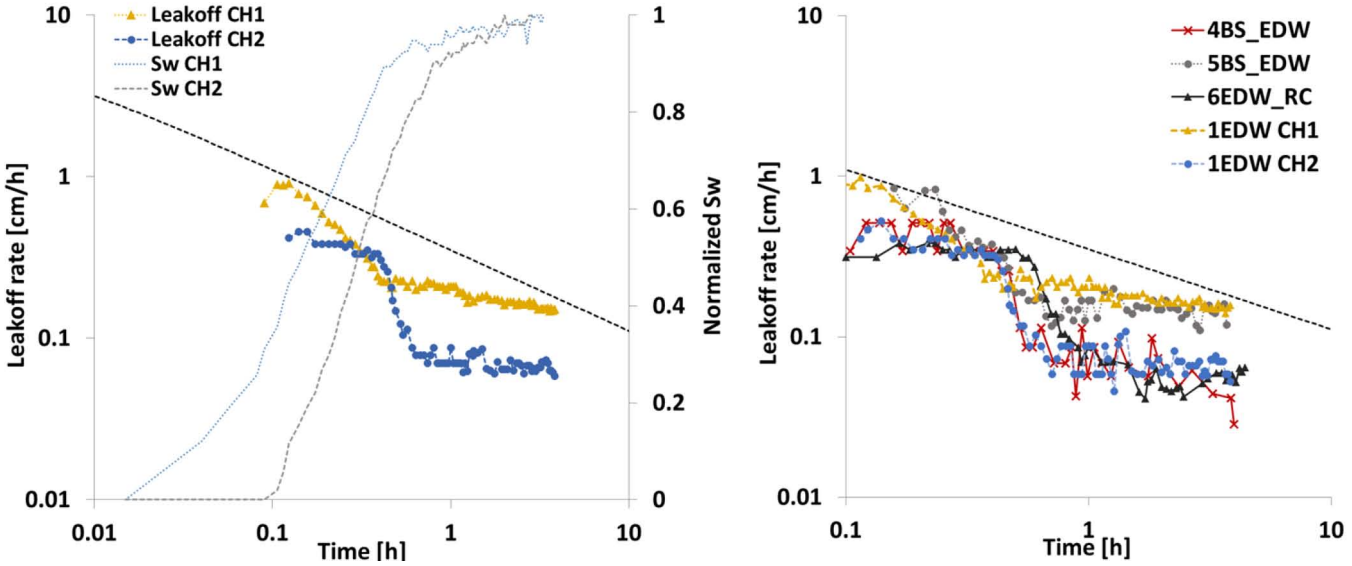

Figure 5—Effluents produced from limestone core halves during gel injection formed the basis for leakoff rate calculations. *Left:*Leakoff rate for core 1EDW (both core halves limestone). *Right:* Leakoff rates for all limestone core halves: limestone coupled with limestone, sandstone and chalk.

Chalk. Rørdal chalk is usually considered to be homogeneous, without significant variations in pore size. **Figure 6** shows the leakoff rates for chalk, calculated from produced effluents from chalk production outlets during gel injection. During early stage gel injection, oil alone was produced from the matrix taps and the leakoff rates followed a decreasing trend similar to the Seright model. At t ~ 0.8h of gel injection, the leakoff rates swiftly decreased, corresponding with the start of two-phase (oil and water) production from the matrix production outlets. From t=1.2, only water was produced out of the matrix taps, and the leakoff rates were nearly constant and lower than expected. Core 3RC was assembled with chalk on both sides of the fracture. The leakoff rates and saturation developments were equal on both sides of the fracture, i.e. the behavior in each core half replicated the other. This could be expected due to the homogeneity of the chalk core material. When chalk was assembled with sandstone (7BS_RC) or limestone (6EDW_RC) on the opposite side of the fracture, the chalk leakoff rates appeared to be influenced by the core material on the other side of the fracture. This is consistent with the observation of oil mainly being produced through the more-permeable core half, as previously discussed.

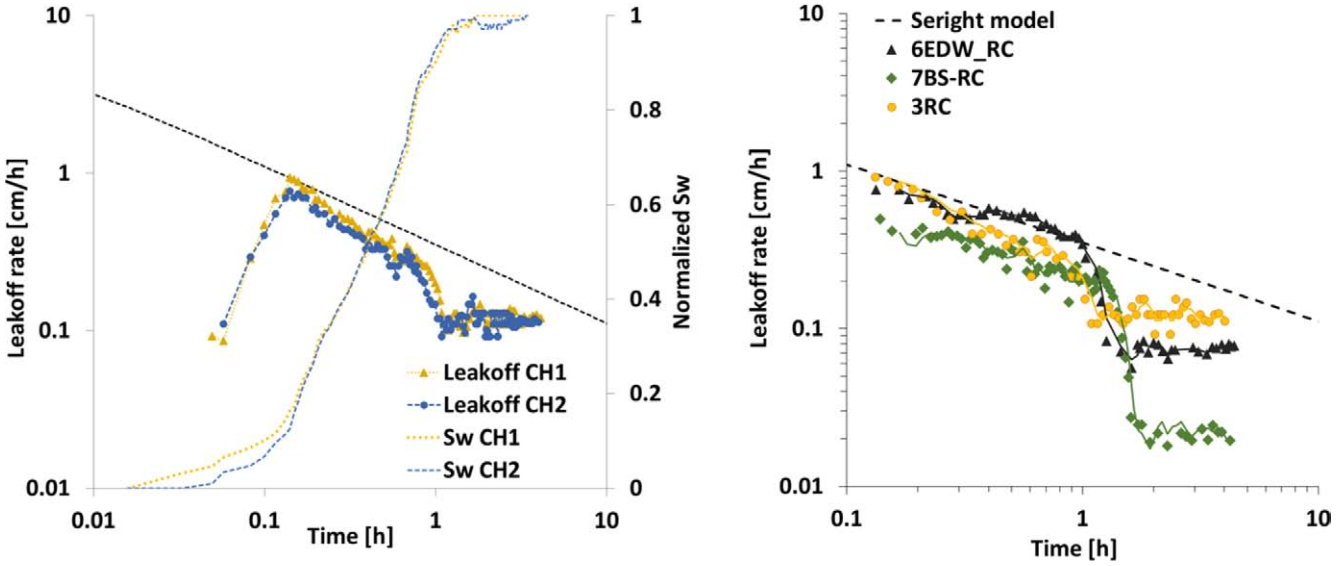

Figure 6—Effluents produced from chalk core halves during gel injection formed the basis for leakoff rate calculations. *Left:*Leakoff in core 3RC (both core halves chalk). *Right:* Leakoff rates for all chalk core halves: chalk coupled with chalk, limestone and sandstone.

Fully water-saturated cores within a range of different permeabilities and pore size distributions were previously used to investigate gel dehydration (see e.g. Seright 2003a), without influencing the measured leakoff rates. In this work, the presence of oil in the rock matrix was observed to influence water leakoff, **Figure 4-6**, where leakoff rates varied with core material and oil saturation. Saturation functions (relative permeability and capillary pressure) are not present in fully water-saturated rocks, but dictate fluid flow in two-phase saturated porous media. Rock properties (e.g., permeability and pore size) strongly influences saturation functions, which may in turn influence gel dehydration.

Understanding the observed leakoff behavior, and interpreting it in terms of saturation and saturation functions, was not straight forward. Magnetic resonance imaging (MRI) was therefore applied to gain insight into *in-situ* fluid flow during gel extrusion through fractures. In chalk, small variations in pore size within the core material was expected, i.e. the capillary pressure varies less with location. A pronounced and reproducible effect on the leakoff behavior was also observed in chalk during initial experiments (**Figure 6**). Rørdal chalk core 8RC was therefore placed in an MRI during gel injection, seeking to understand the apparent impact of oil saturation and core material on leakoff rate.

MRI imaging of gel dehydration in oil-saturated chalk

The leakoff rates presented in **Figures 4-6** were based on volumetric measurements of produced effluents from the matrix during gel injection: the leakoff rate was then calculated by dividing the produced volume by the fracture surface area, and the time increment between measurements. The resulting leakoff rate is given as [distance/time], and can theoretically be related to the velocity of leakoff water passing through a rock matrix. Using MRI, the position of water flowing away from a fracture surface and into an oil-saturated rock matrix can be accurately determined, and its velocity calculated.

Oil-saturated chalk core 8RC was placed in a 4.7 Tesla Biospec MRI to investigate water leakoff during D_2O-gel extrusion through an open fracture. Gel dehydration caused D_2O-brine to leave the gel and invade the rock matrix. The magnetic signal from oil initially in place was removed when the oil was displaced by D_2O. The displacement front was detected by the MRI as the interface between hydrocarbon (signal) and D_2O-brine (no signal), and was recorded with time. Two-dimensional (2D) image slices in the coronal direction (Brattekås and Fernø, 2016) were acquired during D_2O-gel injection in the MRI, to limit acquisition time and accurately capture the water leakoff process. The acquisition time for a coronal slice was 1min

42sec. **Figure 7** shows snap shots of gel injection into core 8RC. The top left corner of the figure shows the initial state of the core, before gel injection started. The bright, white line is bulk oil initially saturating the fracture. The light grey areas are rock matrix saturated by oil. Most of the bulk oil signal in the fracture disappeared when gel started to extrude through the fracture (shown at approximately t=5min), i.e. the oil was displaced. Some of the oil signal, however, remained visible in parts of the fracture. The signal was stable, both in terms of strength and position, throughout gel injection, hence; this was not indicative of counter-current production of oil into the fracture. Further investigations showed that the signal was attributed to oil captured within the gel structure. In experimental work where calculations rely on material balance, the entire bulk volume of oil is expected to be produced from the fracture before gel breakthrough. The departure from this assumption, observed by MRI, can influence the saturation development reported in conventional core scale experiments.

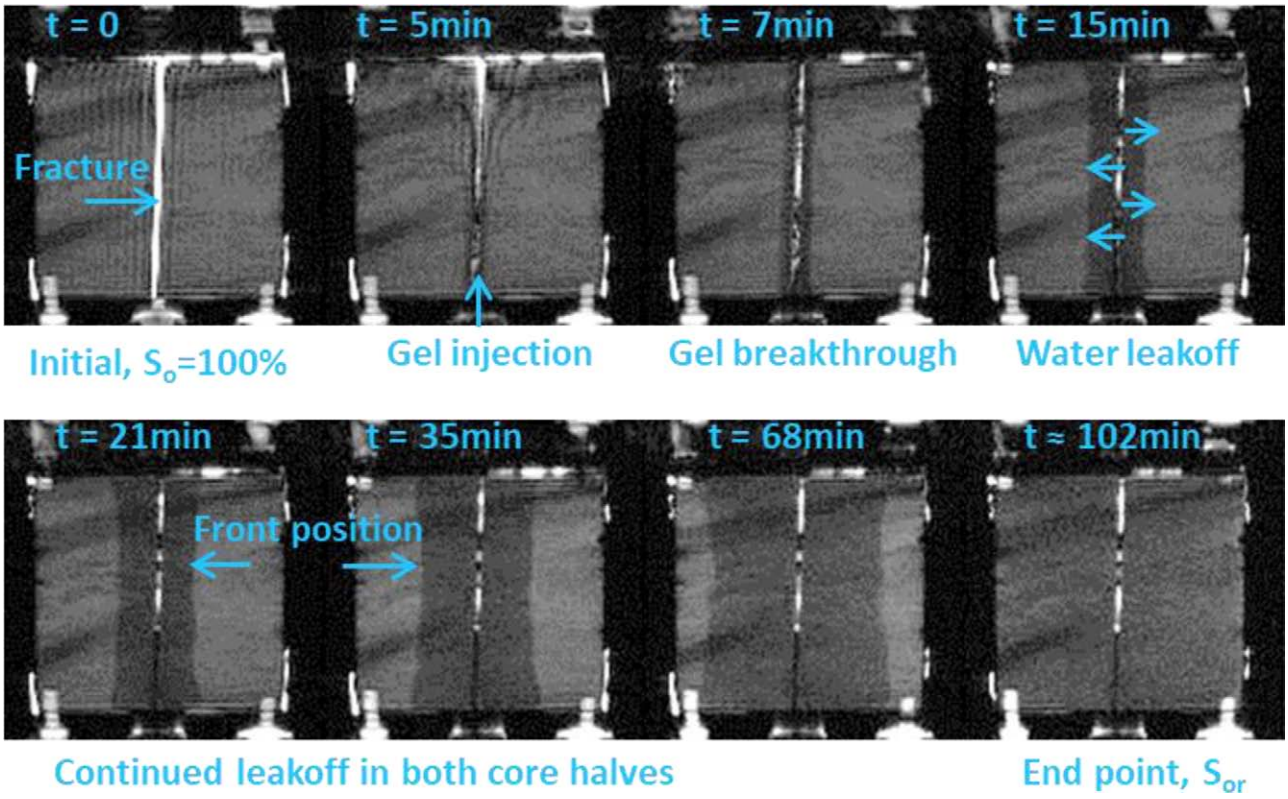

Figure 7—snap shots of solvent leakoff during gel injection into core 8RC, obtained using MRI. The images show the gel dehydration process in the middle of the cylindrical core (top-down).

Gel breakthrough was observed at the fracture outlet at t~ 7 min, after which water leakoff was clearly visible in the rock matrix. The position of the D_2O-water front was identified by MRI at all times, as demonstrated in **Figure 7**: leakoff water may be seen as the dark grey areas in the images, displacing the light grey oil signal away from the fracture surfaces. The leakoff water displaced oil uniformly outwards from the fracture, which suggests that the displacement process in the matrix was strongly influenced by capillary forces. The flow of leakoff water within the matrix was detectable by MRI for as long as oil was dynamically displaced, i.e. during the time line given in **Figure 7**. MRI images acquired during the first 102 minutes of gel injection, during which leakoff could be determined by imaging, were analyzed using basic image analysis software, ImageJ, to extract the front position for several time steps. The velocity of the leakoff water front was then calculated directly by dividing the front location with time.

The velocity of the leakoff water front given by MRI imaging is shown in **Figure 8**. Effluent measurements were only available at designated times during gel injection, due to restrictions in entering

the MRI facilities during imaging; the available leakoff rate points are included in the figure. The leakoff rate based on effluents correspond well with the previous experiments using chalk core material, presented in **Figure 6**. The measured front velocity from MRI imaging does, however, not resemble the leakoff rate calculated from effluent measurements. Nor does it follow the path predicted by the Seright model (although it should theoretically correspond to the [distance/time] parameter given by the model), but yields a higher rate and lower decline versus time. **Figure 8** shows leakoff rates from one experiment, calculated to be both higher and lower than expected, using two different measuring methods. A mismatch between volumetric and directly measured leakoff rates could easily be ascribed as erroneous if reported for different experiments. **Figure 8**, however, shows different leakoff rates for the same leakoff process, where the difference must be attributed to the measuring and calculation methods, and directly related to our understanding of leakoff itself.

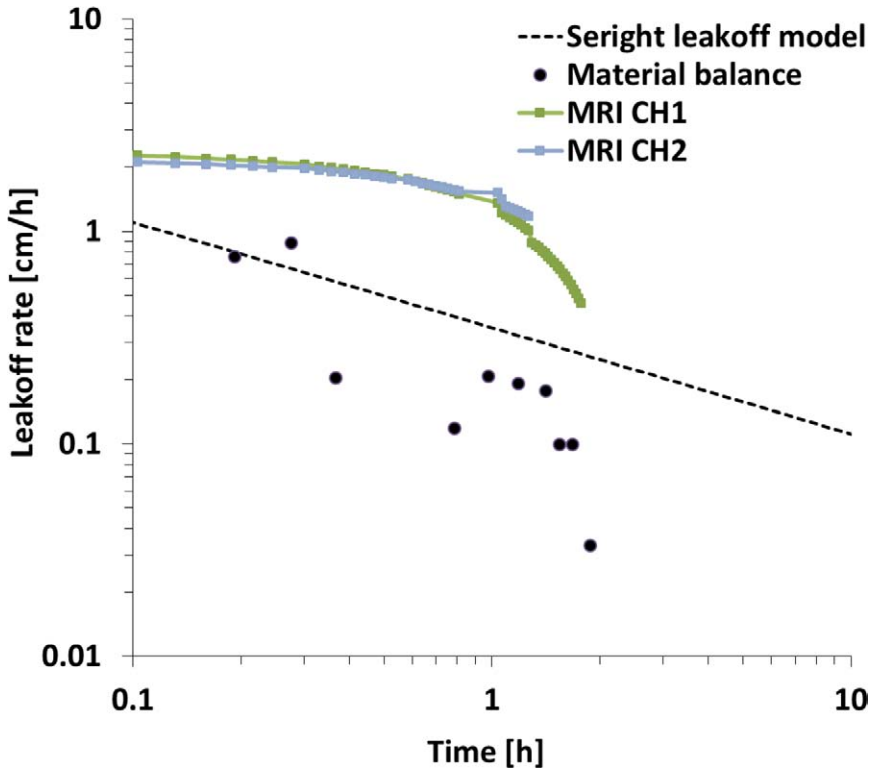

Figure 8—Leakoff rate determined by direct measurements of front location/time by MRI (blue and green lines) compared to leakoff rate calculated from produced effluents (black dots) and the Seright model (black, dotted line).

Water leakoff in cylindrical cores

The commonly used models for leakoff (Seright and Carter) present the leakoff rate as a two-dimensional velocity parameter, although a volumetric flow rate is usually experimentally measured. The conversion of three-dimensional, volumetrically measured data (the effluents) to a two-dimensional parameter describing velocity has this far been unproblematic: experiments have repeatedly shown that the leakoff rate corresponds with the models (measured to be linearly decreasing on a log-log plot of leakoff rate versus time), despite of significant experimental variability. Cores of different rock materials, shapes and dimensions have been used, and gel injected using a variety of injection rates and volumes. Dividing the produced fluid volume by the fracture surface area and time increments between measurements to calculate the leakoff rate has provided reproducible results.

In this work, imaging by MRI provide insight to the flooding process within the rock matrix. We observed that water leaking off into oil-saturated chalk formed a uniform displacement front through the core matrix. The distance from the fracture to the leakoff front was equal for all core lengths, i.e.; one velocity could be

assigned to the front. Volumetric measurement of effluents (3D) can, therefore, be related to the velocity of the fluid front (2D) in this specific core, although only theoretically in previous work. To correctly relate the leakoff water front position measured by MRI to a fluid volume, the MRI images must be corrected for:

1. Porosity: the area behind the leakoff front holds rock material in addition to fluids.
2. Residual oil saturation (S_{or}): the pore space was initially saturated by oil. Although some of the oil is displaced by water, residual oil resides behind the leakoff front position and occupies parts of the pore volume.

Figure 9 shows a schematic of gel dehydrating in an open fracture, forcing water into the matrix to displace oil, and illustrates an additional correction necessary when using cylindrically shaped cores: the volume of oil ahead of the leakoff front will decrease as the front moves closer to the core circumference. I.e. when leakoff water flows into the rock matrix close to the fracture surface it will displace more oil than when flowing a corresponding distance further into the rock matrix.

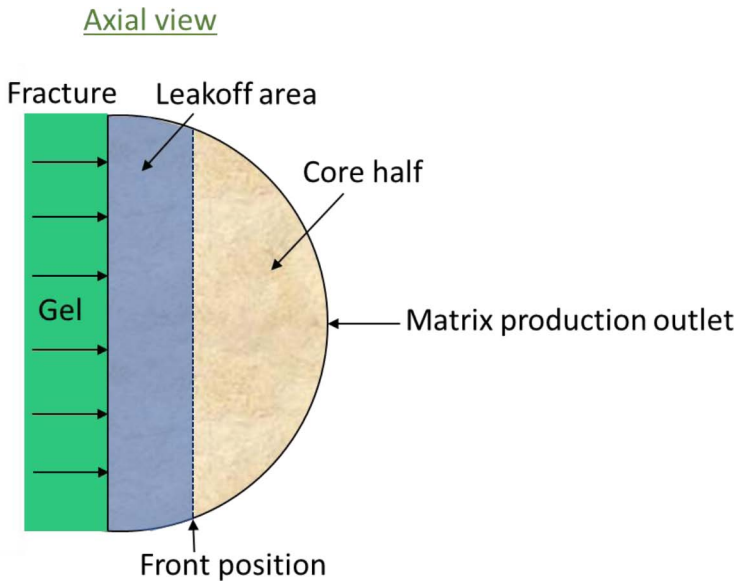

Figure 9—Axial view of gel dehydration in an open fracture. The front position (penetration distance of leakoff water into the matrix) was measured using MRI.

The argument of a uniform leakoff front with a single velocity, validated by MRI, was used to modify the Seright model to reflect the cylindrical shape of core 8RC:

Step 1: a theoretical leakoff distance was calculated for designated time steps (the leakoff rate given by the Seright model [cm/h], was multiplied by time to provide the leakoff distance).

Step 2: Simple trigonometry was used to find the leakoff area (**Figure 9**: the area behind the leakoff front) for each calculated leakoff distance.

Step 3: The leakoff area was multiplied with the fracture length for each time step. This provides a volume, which can be converted to a leakoff rate through conventional calculations (dividing the volume by fracture surface area and time increments). The converted leakoff rate provided by the Seright model and the dimensions and shape of core 8RC is shown in **Figure 10** (orange line).

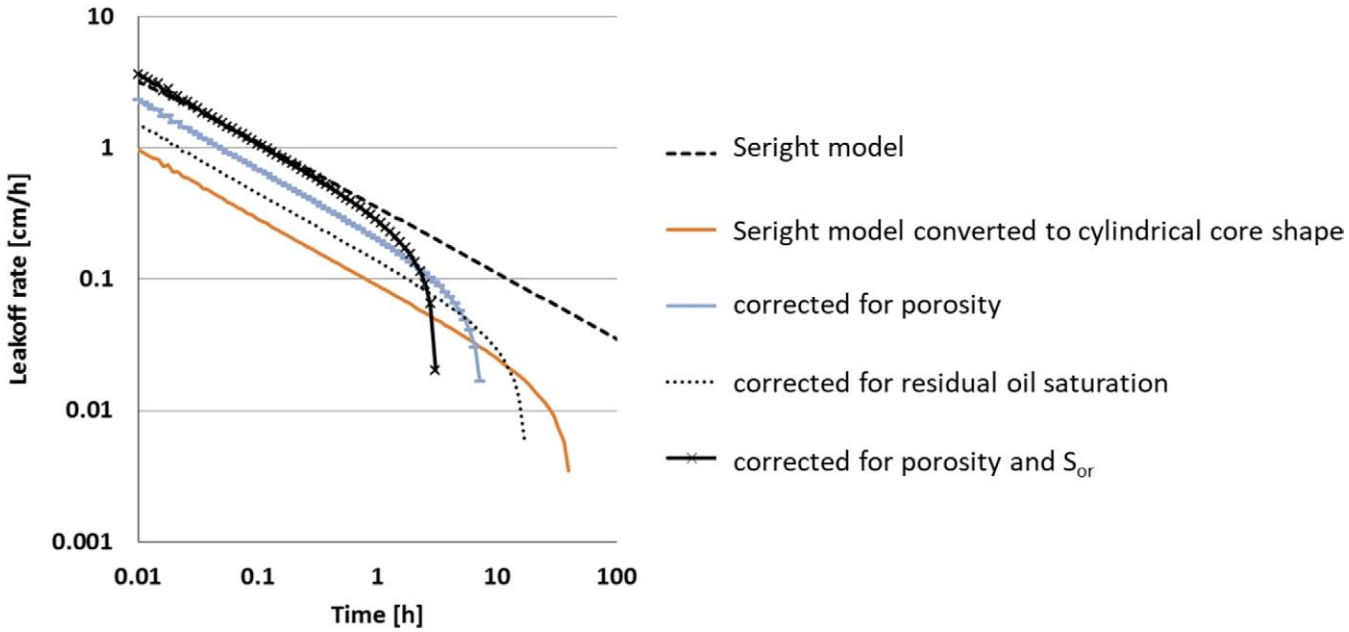

Figure 10—Modified model for leakoff in an oil-saturated cylindrical chalk core (orange) corrected for S_{or} (black, dotted line), porosity (blue line), and S_{or} and porosity (black crosses). Note that the core diameter for these curves is fixed at 4.6cm, corresponding to core 8RC.

Step 4: The modified model was corrected for estimated porosity (blue line) and residual oil saturation (dotted, black line), respectively, to review their separate impacts. To correctly reflect gel injection into an oil-saturated chalk core, the model must be corrected for both.

A modified Seright model, corrected for core shape, porosity and saturation is shown as black crosses in **Figure 10**. The modified model reflects the fluid volume displaced by the front at any given time step, and thus provides the leakoff rate expected from volumetrical measurements (effluents) in cylindrical Core 8RC. Gel injection into oil-saturated chalk cores (**Figure 6**) is well captured by the modified model: a high leakoff rate, close to the original Seright model, can be expected initially. The leakoff rate decline is faster than originally anticipated, with a sudden swift decrease. The swift decline in leakoff rate appear when the leakoff front reaches the matrix production outlets located at the core circumference. When the leakoff front approaches the core circumference, the volume of oil ahead of the front very quickly diminishes, which is reflected in a smaller volume produced from the matrix. In many cylindrical cores, leakoff rates measured from effluents have corresponded well with the conventional Seright model (e.g. Brattekås et al (2015), oil-saturated sandstone, **Figure 4**). In such cases, a stable displacement front with one representative velocity cannot exist.

Figure 11 compares the modified leakoff model to the leakoff front velocity in (measured by MRI and corrected for porosity and residual oil saturation) and volumetric effluent measurements, respectively. Taking the core shape into account significantly improves the match between model and measurements. The swift decline in leakoff rate observed in volumetric measurements, and confirmed by MRI imaging, appear when the leakoff front approaches the core circumference, and is captured by the model. The transient period (two-phase production) occurs when the front reaches the production outlets, and was short in chalk. The displacement front cease to exist when the transient period is over, and leakoff water is produced through the production outlets.

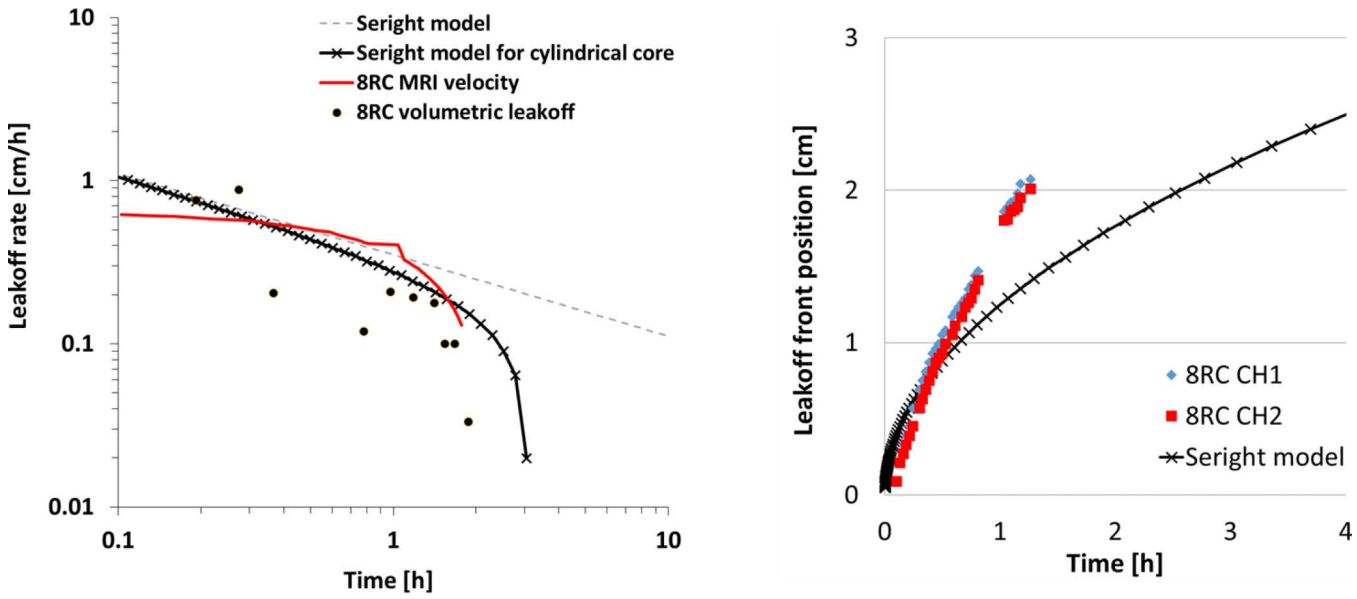

Figure 11—*Left:*leakoff rate from MRI imaging (red line), compared to the expected leakoff rate for core 8RC based on the Seright model (black crosses) and the volumetrically calculated leakoff rate (black dots). *Right:* the leakoff water front position of core 8RC measured by MRI compared to leakoff distance calculated directly from the Seright model. The front position was corrected for porosity and S_{or}.

The position of the leakoff front measured by MRI compared to the theoretical leakoff distance given directly by the Seright model (see *Step 1* above) is shown in **Figure 11** (Right). The leakoff water front position measured by MRI initially reached a shorter distance into the rock than predicted by the Seright model. The declining development of the leakoff front position predicted by the Seright model was, however, not reflected in the MRI measurements, and from t = 0.39 h, the leakoff front moved faster in core 8RC, and reached further into the rock than anticipated. Note that the core shape is not accounted for in the leakoff front position given by the Seright model, which may cause these deviations.

MRI imaging of water chase flood

After gel injection, H_2O-brine (composition corresponding to the D_2O-brine used as solvent) was injected into core 8RC. Unlike the D_2O-brine used for gel solvent, H_2O-brine provides a signal detectable by MRI. The gel rupture pressure was measured at 15.7 psi/ft, which corresponds well with previously measured rupture pressures at the same gel injection rate and throughput (Brattekås et al., 2015). After gel rupture, water may pass through the gel-filled fracture. **Figure 12** shows a 3D image of core 8RC during waterflooding. The matrix was at S_{or} during waterflooding, with D_2O constituting the water phase. The majority of signal was therefore detected in the fracture. Two fluids were responsible for the signal: oil coating the gel (purple color in **Figure 12**), and H_2O-brine flowing through the gel (yellow color). The H_2O-brine was distinguishable from the oil phase by proper thresholding of the MRI images. Water flow through the gel-filled fracture was observed to occur in narrow flow channels, often termed *wormholes*. The wormholes appear randomly distributed in the fracture, which support the Seright model description of a randomly distributed filter cake in the fracture volume.

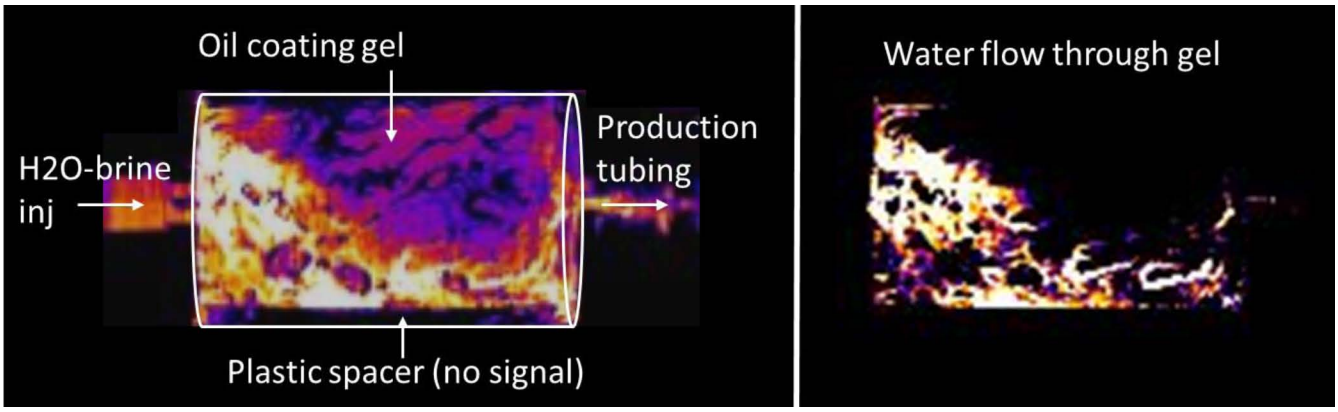

Figure 12—H_2O-brine injection into the gel-filled fracture of core 8RC. *Left:* 3-D image of the core. The signal shown comes from the fracture only. The purple signal is oil coating the gel. *Right:* with proper thresholding, the signal from H2O-brine can be distinguished. Water moves through the gel-filled fracture through a network of narrow flow channels (*wormholes*).

Current experimental work in context: Should the leakoff rate correspond to front velocity?

Previous leakoff experiments have repeatedly shown that gel dehydration follows the same trend, accurately described by the Seright model, in core systems of different core materials, shapes and dimensions. In this work, we observed that the leakoff rate was determined by conditions behind and ahead of the fluid displacement front (**Figure 10** and **Figure 11**), which challenge the idea of a global prediction of leakoff rate.

In experiments where the rock matrix is saturated by one phase only (often water), matrix flow is controlled by absolute permeability, given by Darcy's law. Water can flow into the matrix at any location, provided that the matrix permeability exceeds the permeability of the gel in the fracture. It is highly likely that the leakoff process is controlled by the properties of gel and where it resides (the fracture properties) in such cases, while the rock matrix acts like a filter for the gel. Our current observations propose that water leakoff is not controlled by the gel alone in all systems, but also impacted by saturation functions in the rock matrix when oil is present. A uniform leakoff front outwards from the fracture was observed in a chalk core by MRI. The unique velocity of the leakoff front rendered modification of the Seright model possible, to accurately capture the experimental properties (e.g. core shape) and improve the match between model and experiments. Because the modifications to the leakoff model depends on the properties of the experiment, the same leakoff rate cannot be expected for varying core shapes, saturations and, above all, wettabilities.

Leakoff was originally defined as a filtration velocity at the fracture surface, which may not be easily measured in conventional core scale experiments. Using imaging methods to directly measure the position of the leakoff front in a porous rock should give a close approximation to the filtration velocity. Such measurements will, however, be influenced by differences in porosity (also for fully water saturated rocks), and residual saturations. Further, the correlation between volumetric measurements and a filtration velocity depends on the fluids passing through a uniformly shaped media, which is not the case when using cylindrical cores. Although the notion of leakoff rate as a filtration velocity at the fracture surface is initially logical, the presentation of leakoff rate as [distance/time] based on [volume/time] measured data may be dubious: water that passes from the gel through the fracture surface will not always propagate unhindered through any rock, and our measuring methods and understanding of the term "leakoff rate" will impact the results and our interpretation of the results, respectively. This was emphasized by the initial deviation between the directly (2D) and volumetrically (3D) measured leakoff rates in a cylindrical core shown in **Figure 8**. MRI imaging of gel injection into oil-saturated chalk core 8RC showed that water displaced oil in a piston-like manner, uniformly outwards from the fracture surface, i.e. the front had one representative velocity. This may be attributed to the strong capillary forces in chalk, and may not be used as a global assumption for all core systems. However; for core 8RC, and probably for similar chalk cores, this observation connected volumetric measurements of leakoff rate to a unique leakoff distance, and the

Seright model could be modified. When saturation functions are less influential of flow (e.g. sandstone), or non-existing (water saturated cores), matrix flow will to a larger extent be controlled by the pressure drop between the gel in the fracture and the matrix production outlet, and more likely to vary with fracture length. A uniform displacement front outward from the fracture is less likely to form in such systems. We may therefore question whether we should expect the volumetrically measured leakoff rate to correspond to a leakoff distance in these cases. We argue that the volume of water leaving the gel is more important for most applications than how far into the matrix, and how fast, the water is moving. The volume of water leaking off from the gel controls the rate of gel propagation into a reservoir, as well as the degree of gel dehydration and fracture growth during hydraulic fracturing, and is measured directly in most conventional experiments. The presentation of leakoff rate as a two-dimensional parameter may be useful to normalize the experimental data and remove the impact of fracture volume (which is significantly different in previous experiments) on leakoff rate. The "normalized" leakoff rate is an average for the entire fracture, where variations in gel dehydration within the fracture volume are not accounted for. Although this "normalized" leakoff rate may be used to compare leakoff experiments to the Seright and Carter models, it may not be assumed to represent a unique velocity, or a leakoff distance, in the rock matrix in most experiments.

Gel dehydration on the core scale

The current work shows that the volume of water leaving gel (here understood as the leakoff rate) during extrusion through fractures depends on the conditions of the rock matrix: e.g. its shape and saturation. **Figure 4-6** also indicated leakoff dependency on core material, with more pronounced deviations in high capillarity core materials like chalk and limestone. A significant difference between water displacement in oil-saturated chalk and oil-saturated sandstone is the development of a stable and capillary driven displacement front in chalk. The forming of a stable displacement front (verified by MRI imaging in core 8RC) combined with the core shape explained the reproducible deviations from expected leakoff in the chalk cores, illustrated in **Figure 13**. Relative permeability and capillary pressure curves representative of the chalk core material are also shown in the figure. Gel injection started at zero water saturation ($S_w = 0$), i.e. 100% oil saturation. Strong capillary forces could impact the leakoff process at high oil saturations (accelerate or slow down, depending on the balance between capillary and viscous forces), becoming lower and less controlling of the process at low oil saturations. Previous work (Brattekås et al, 2014) showed that capillary forces in chalk at strongly water-wet conditions could dehydrate polymer gel and reduce its volume by up to 98%. Another previous study by the authors and others (Brattekås et al, 2013) also indicated an influence of oil-wet conditions on gel dehydration: using CT imaging, we observed that the water saturation in the matrix of an oil-wet limestone did not change during gel injection, i.e. leakoff water did not enter the matrix when gel was injected at a low injection rate. Increasing the gel injection rate, and thus the differential pressure across the fracture, allowed leakoff close to the inlet end of the core, verified by an increasing water saturation in the inlet end of the matrix. The pressure drop was not sufficient to allow water to travel the length of the matrix; and the water re-entered the gel-filled fracture to be produced through the fracture outlet. Hence: volumetric measurements of effluents in core scale experiments may not always correctly reflect fluid flow within the system, and separate measurements of fracture and matrix flow do not ensure continuous transportation of the measured fluid through either. The use of small, strongly wetted, core plugs in the present study also influenced the saturation development within each core half (***Gel injection into fractured, oil-saturated core plugs***).

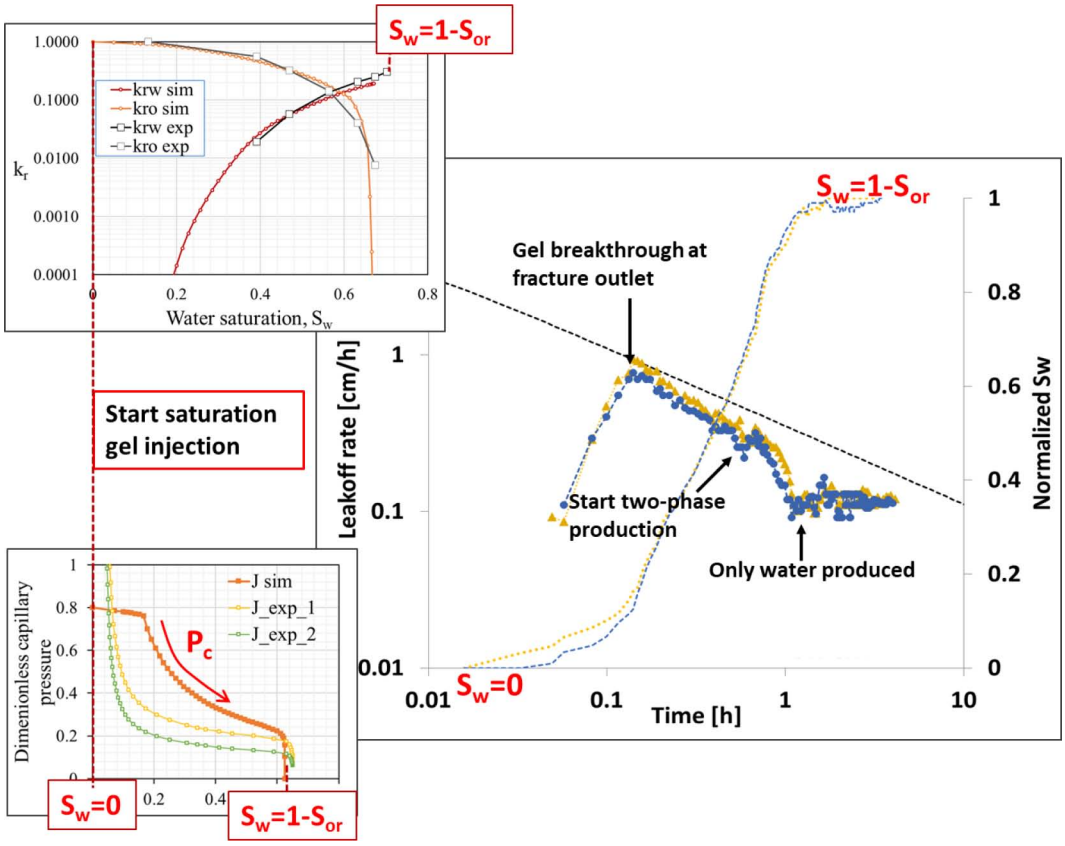

Figure 13—The volumetrically measured leakoff rate deviated from the Seright model in oil-saturated limestone and chalk cores. The leakoff behavior was consistent: high initial leakoff, but swiftly reduced during two-phase production. At the end of two-phase production, water alone was produced from the matrix, and the leakoff rate was close to constant. The relative permeability and capillary pressure curves shown on the left are representative of the chalk core material. The saturation at the start of gel injection was S_w = 0. The figures were modified from Andersen *et al.* (2018).

At the residual oil saturation, S_{or}, capillary forces no longer aid (or limit) leakoff; the flow of water through the matrix is then controlled by the end-point relative permeability to water, $k_{rw,or}$ (flow within the rock matrix) and the gel (inflow of water to the matrix from gel). Leakoff in chalk, and its deviation from the conventional leakoff model, is shown in **Figure 13**. A significant deviation between the expected and measured leakoff was observed at S_{or}, which cannot be related to the core shape or a capillary driven displacement front. Although flow within the matrix is limited by k_{rw}, this may not be the only explanation for the deviation: strong capillary forces in the matrix (previously observed to reduce the gel volume by up to 99% without applying additional pressure on the gel, Brattekås et al (2014)) could influence filter-cake formation in the adjacent fracture during gel injection, possibly drawing the gel closer and more evenly to the fracture surface, and increasing the contribution to leakoff from the dehydrated gel layer. Both these effects limit the number of leakoff sites during late-stage gel injection, which can reduce the leakoff rate.

It is also possible that leakoff may be influenced by the experimental setup, specifically the use of 1/8'' tubings drilled into the cores at the core circumference to represent the production outlet for both oil and water. The outlet was small relative to the leakoff area (fracture surface), and inflow of two fluid phases into the small area around the production tubing may cause a "choke effect", where each fluid limits the flow of the other. This hypothesis was tested in chalk, by implementing different production outlet designs, but no evidence of a choke effect was observed: the original 1/8'' outlets were therefore used in the sandstone cores. In the current work, MRI imaging showed that leakoff in chalk was controlled by the formation of a displacement front, and less so by outlet properties. This was, however, not true for sandstone, where the magnitude and direction of the viscous pressure drop (implemented by gel) controls the majority of matrix flow. An influence of outlet properties may explain the lower than expected leakoff rates in oil-saturated

sandstone. Influences from outlet properties, e.g. from using 1/8'' tubings as matrix production outlets, are more likely to occur in cores where the displacement front is non-existing or less influential on fluid flow.

Deviations from conventional and expected leakoff behavior observed when the rock matrix is saturated by two phases instead of one can be attributed to saturation functions (e.g. a high capillary pressure causing the formation of a stable displacement front), properties of the gel (e.g. limited leakoff-sites) and/or properties of the experiment (e.g. cylindrical core shape, outlet properties). Analyzing leakoff when gel dehydration is not solely dictated by gel or fracture properties must be done while considering possible influences from both the matrix, gel and the experiment. Gel dehydration is influenced by both the gel/fracture properties and the matrix when capillary forces balance or overcome the viscous forces applied by gel, i.e. using two-phase saturated rocks of strong wetting preference. This work indicated that the leakoff rate depends on whether or not a displacement front forms in the matrix, in addition to a demonstrated effect of e.g. core shape. The discussion comprised several factors that render core scale experiments and reliable subsequent analysis challenging, especially in conventional experiments without imaging. A good example is the swift drop in leakoff observed during gel injection in oil-saturated chalk: this behavior is not a general characteristic of leakoff in oil-saturated chalk, nor can it be expected in all experiments: it is simply attributed to the presence of a stable displacement front moving through a non-uniformly shaped medium. Using this or similar experimental results to represent leakoff on larger scales, e.g. during gel injection in a chalk reservoir, would not be advisable.

Upscaling to field applications.

Reservoir rock is frequently saturated by more than one fluid, and fluid transport in fractured reservoirs, especially in low-K rock formations, rely on capillary forces. The shape of matrix blocks is not always uniform, and the wettability of the rock formation may have changed during ages of crude oil exposure. Hence: reservoirs, that could be suitable candidates for polymer gel treatments, can exhibit several of the factors identified in this work to influence leakoff. The conventional Carter and Seright leakoff models are based on water-saturated, high-K rock, where the leakoff behavior is most likely controlled by the properties of the gel and fracture network. In the near-well area, due to high viscous pressure gradients, leakoff may be determined by gel and the conventional models correct. Basing enitre reservoir predictions on these models may, however, fail to capture the true properties of many in-depth polymer gel treatments. The challenge is further complicated by the pit-falls of core scale analysis identified in this work, where lab experiments without imaging could easily be misinterpreted. Good and representative modelling of gel behavior, and validation of controlled core scale experiments with both imaging and modelling, is a possibility to overcome these challenges and improve predictions. Initial modelling of gel behavior during spontaneous imbibition is presented in Andersen et al. (2018).

Conclusions

- The leakoff rate must be clearly defined. For most applications, the volume of water leaving the gel is most important; this controls the rate of gel propagation into a reservoir and fracture growth during hydraulic fracturing. The representation of this leakoff rate as a two-dimensional parameter is useful, to account for variations in fracture volume between experiments.
- The leakoff rate is most often not a velocity. In some experiments, leakoff water forms a stable displacement front parallel to, and moving away from, the fracture, and the volumetric leakoff rate can be related to a velocity. Imaging must be applied to validate this relation.
- MRI was successfully used to track the leakoff front position during gel injection into oil-saturated chalk, and identified the existence of a stable and capillary driven displacement front in the rock matrix.

- The swift decline in leakoff rate observed in oil-saturated chalk cores was verified by MRI, and explained by the non-uniform shape of the rock matrix through which the leakoff displacement front moves. The volume ahead of the front quickly diminishes, which lead to less produced oil. This behavior must not be mistaken for a general characteristic of leakoff in oil-saturated chalk.
- Saturation functions in the rock matrix can influence leakoff. We propose that leakoff deviates from conventional behavior when capillary forces in the matrix balance the viscous force applied on the system by gel. Positive capillary forces may support the formation of a stable displacement front in the matrix. Negative capillary forces (oil-wet preferences) may prevent leakoff water from entering the matrix. The leakoff rate will then no longer be controlled by gel only.
- Gel dehydration on the core scale must be analyzed while considering influences from the matrix (e.g. saturation functions, wettability), the gel (e.g. filter-cake formation, leakoff sites) and experimental properties (e.g. core shape, outlet properties)
- The rock matrix of a productive oil reservoir is often saturated by (at least) two phases. Leakoff during gel injection into real reservoirs may also be influenced by these factors. Representative numerical modeling of the gel, and gel/rock matrix interactions may provide improved core- and reservoir-scale predictions.

Acknowledgements

MR Imaging was performed at the Statoil MRI Research Centre at Sandsli, Bergen. The authors acknowledge Per Fotland for his valuable help during experiments.

The authors acknowledge the Research Council of Norway and the industry partners; ConocoPhillips Skandinavia AS, Aker BP ASA, Eni Norge AS, Maersk Oil Norway AS, DONG Energy A/S, Denmark, Statoil Petroleum AS, ENGIE E&P NORGE AS, Lundin Norway AS, Halliburton AS, Schlumberger Norge AS, Wintershall Norge AS of The National IOR Centre of Norway for support.

Nomenclature

L – length of core half
H – height of fracture
r_{max} – the maximum thickness of a core half (minimum distance between fracture and matrix production outlet)
CH1, CH2 – core half 1, core half 2
K_{ratio} – the approximate permeability contrast between the core halves of a fractured system
mL/h – milliliters per hour, rate of fluid injection or production
S_i – Saturation
Subscript i – oil (o) or water (w)
S_{wi} – Irreducible water saturation
S_{or} – Residual oil saturation
k_{ri} – Relative permeability of i
P_c – Capillary pressure
POM – Polyoxymethylene

References

Andersen, P.Ø., Lohne, A., Stavland, A., Hiorth, A. and Brattekås, B. (2018). "Core Scale Simulation of Spontaneous Solvent Imbibition from HPAM Gel". SPE Improved Oil Recovery Conference, Tulsa, OK, USA.

Brattekås, B., Haugen, Å., Ersland, G., Eide, Ø., Graue, A. and Fernø, M.A. (2013). "Fracture Mobility Control by Polymer Gel- Integrated EOR in Fractured, Oil-Wet Carbonate Rocks". EAGE Annual Conference & Exhibition incorporating SPE Europec. London, UK.

Brattekås, B., Haugen, Å., Graue, A., Seright, R. (2014). "Gel Dehydration by Spontaneous Imbibition of Brine from Aged Polymer Gel". *SPE Journal*, **19**(1), 122–134. https://doi.org/10.2118/153118-PA

Brattekås, B., Pedersen, S.G., Nistov, H.T., Haugen, Å., Graue, A., Liang, J-T. and Seright, R.S. (2015). "Washout of Cr(III)-Acetate-HPAM Gels From Fractures: Effect of Gel State During Placement". *SPE Production & Operations.* **30**(02): 99–109.

Brattekås, B., Graue, A., Seright, R.S. (2016). "Low-Salinity Chase Waterfloods Improve Performance of Cr(III)-Acetate Hydrolyzed Polyacrylamide Gel in Fractured Cores". *SPE Reservoir Evaluation & Engineering.* **19**(02): 331–339.

Brattekås, B. and Fernø, M. A. (2016). "New Insight from Visualization of Mobility Control for Enhanced Oil Recovery Using Polymer Gels and Foams". *Chemical Enhanced Oil Recovery (cEOR) – a Practical Overview. L. Romero-Zêron, InTech*

Dantas, T. N. C., Santanna, V.C., Dantas Neto, A.A., Alencar Moura, M.C.P. (2005). "Hydraulic Gel Fracturing". *Journal of Dispersion Science and Technology* **26**(1): 1–4.

Ekdale, A. A. and R. G. Bromley (1993). "Trace Fossils and Ichnofabric in the Kjølby Gaard Marl, Uppermost Creataceous, Denmark". *Bull Geol. Soc. Denmark* **31**: 107–119.

Haugen, Å., Fernø, M.A. and Graue, A. (2008). "Numerical simulation and sensitivity analysis of in-situ fluid flow in MRI laboratory waterfloods of fractured carbonate rocks at different wettabilities". SPE ATCE, Denver, CO, USA.

Hild, G. P. and R. K. Wackowski (1999). "Reservoir Polymer Gel Treatments To Improve Miscible CO2 Flood". *SPE Reservoir Evaluation & Engineering* **2**(02): 196–204.

Hjuler, M. L. and I. L. Fabricius (2007). "Diagenesis of upper creatceous onshore and offshore chalk from the North Sea area". Kgs. Lyngby: DTU Environment.

Howard, G. C. and C. R. Fast (1957). "Optimum Fluid Characteristics for Fracture Extension". *Drilling and Production Practices*. API(261).

Howard, G. C. and C. R. Fast (1970). "Hydraulic Fracturing". Richardson, Texas, SPE.

Johannesen, E. B. (2008). "NMR characterization of wettability and how it impacts oil recovery in chalk". *Dept. of Physics and Technology*. Bergen, University of Bergen. **PhD thesis:** 71.

Kantzas, A., Allsopp, K. and Marentette, D. (1999). "Utilization of Polymer Gels, Polymer Enhanced Foams, And Foamed Gels For Improving Reservoir Conformance". *Journal of Canadian Petroleum Technology* **38**(13).

Klein, E. and T. Reuschle (2003). "A Model for the Mechanical Behaviour of Bentheim Sandstone". *Pure applied Geophysics* **160**: 833–849.

Liu, J. and R. S. Seright (2001). "Rheology of Gels Used for Conformance Control in Fractures". *SPE Journal* **6**(02).

Penny, G. S. and M. W. Conway (1989). "Fluid Leakoff", Recent Advances in Hydraulic Fracturing". Richardson, Texas, SPE.

Portwood, J. T. (2005). "The Kansas Arbuckle Formation: Performance Evaluation and Lessons Learned From More Than 200 Polymer-Gel Water-Shutoff Treatments". SPE Productions and Operations Symposium. Oklahoma city, OK, USA.

Schutjens, P. M. T. M., Hausenblas, M., Dijkshoorn, M. and Van Munster, J.G. (1995). "The influence of intergranular microcracks on the petrophysical properties of sandstone- experiments to quantify effects of core damage". International Symposium of the Society of Core Analysts, San Francisco, CA.

Seright, R. S. (1995). "Gel Placement in Fractured Systems". *SPE Production & Facilities* **10**(4): 241–248.

Seright, R. S. (1999). "Polymer Gel Dehydration During Extrusion Through Fractures". *SPE Production & Facilities* **14**(2): 110–116.

Seright, R. S. (2001). "Gel Propagation Through Fractures". *SPE Production & Facilities* **16**(4): 225–231.

Seright, R. S. (2003a). "An Alternative View of Filter-Cake Formation in Fractures Inspired by Cr(III)-Acetate-HPAM Gel Extrusion". *SPE Production & Facilities* **18**(1): 65–72.

Seright, R. S. (2003b). "Washout of Cr(III)-Acetate-HPAM Gels from Fractures". International Symposium on Oilfield Chemistry. Houston, TX, Society of Petroleum Engineers.

Seright, R. S., Lane, R.H. and Sydansk, R.D. (2003c). "A Strategy for Attacking Excess Water Production". *SPE Production and Facilities* **18**(03): 158–169.

Sydansk, R. D. and G. P. Southwell (2000). "More Than 12 Years Experience With a Successful Conformance-Control Polymer-Gel Technology". *SPE Production & Operations* **15**(4): 270–278.

Tie, H. (2006). "Oil Recovery by Spontaneous Imbibition and Viscous Displacement from Mixed-Wet Carbonates". *Department of Chemical and Petroleum Engineering*. Laramie, Wyoming, The University of Wyoming. **PhD thesis:** 238.

Willhite, G. P. and R. E. Pancake (2008). "Controlling Water Production Using Gelled Polymer Systems". *SPE Reservoir Evaluation & Engineering* **11**(3): 454–465.